SPACE TELESCOPE SCIENCE INSTITUTE
Operated for NASA by AURA

Instrument Science Report ACS 2013–03

ACS/WFC Geometric Distortion: a time dependency study

Leonardo Úbeda, Vera Kozhurina-Platais
Space Telescope Science Institute
Luigi R. Bedin
Osservatorio Astronomico di Padova
August 26, 2013

ABSTRACT

We re-visit the issue of the time-dependency variation of the linear terms in the ACS/WFC *geometric distortion. We performed a detailed photometric/astrometric study using* F606W _FLT *and* _FLC *images from the calibration field near globular cluster 47 Tucanae. We analized the time dependency of the linear terms by comparing individual observations with a standard catalog. A previous calibration of these drifts proved to be able to restore positions to the milli-arcsecond level for pre-SM4 data. We confirm this previously existing solution and we provide new and simple corrections for both* _FLT *and* _FLC *images that will allow observers to perform global astrometric studies with 0.02* WFC *pixel precision using both pre- and post-*SM4 *images.*

1. Introduction

The Hubble Space Telescope (HST) Advanced Camera for Surveys (ACS) Wide Field Camera (WFC) consists of two 4096×2048 charge-coupled devices (CCDs), which are butted together along their long dimension to create an effective 4096×4096 array. Images obtained using the

ACS/WFC suffer from strong geometric distortion: the square pixels of its detectors project on the sky as parallelograms.

High-precision astrometry with HST could be achieved with an accurate modeling of this geometric distortion. The original studies involving the ACS/WFC were performed by Meurer *et al.* (2002) and Anderson (2002). Both papers show that the distortion of the ACS/WFC detectors is highly non-linear and that a fourth order polynomial is adequate for characterizing the distortion to an accuracy better than the 0.2 pixel requirement. A look-up table for each filter is requiered to achieve 0.01 WFC pixel accuracy

In 2004, during reduction of the Hubble Ultra Deep Field, it was noticed that there was a problem with the alignment of images obtained at different orientations. This led to the discovery that the linear terms in the distortion solution have changed monotonically since ACS was installed in 2002. An empirical time-dependent correction for these drifts was found by Anderson (2007) using hundreds of ACS/WFC images of the calibration field of 47 Tucanae obtained between 2002 and 2006. Anderson (2007) produced an accurate 47 Tucanae reference frame with a nominal scale of 0.050 "/pixel, as well as an improved master source catalog (`ALLSTAR.RIGID.XYM`) with $\sim 53\,000$ sources found in the field.

Soon after Servicing Mission 4 (SM4, which took place on 12 May 2009), it was realized that the behaviour of the linear terms derived in Anderson (2007) might no longer be valid for post-SM4 data.

The goal of this Instrument Science Report is to revise the pre-SM4 linear terms of the ACS/WFC distortion solution using both `_FLT` and `_FLC` images and to derive an empirical correction of time-dependency in the linear terms for post-SM4 distortion.

2. The Linear Terms

The standard astrometric procedure to examine the accuracy of the geometric distortion is to compare the position of stars corrected for distortion on a measured frame with the positions of the same stars in a distortion-free reference frame. The residuals between the observed positions of stars and the corresponding positions in the astrometric standard catalog reveal the accuracy of the distortion. For the present work, we adopt the catalog `ALLSTAR.RIGID.XYM` derived by Anderson (2007).

According to Anderson (2007), to map the positions from a distortion-corrected frame $(x_{\rm corr}, y_{\rm corr})$ into a distortion-free astrometric flat-field $(\mathcal{X}, \mathcal{Y})$ one could use a linear transformation with six parameters as the following:

$$\begin{pmatrix} \mathcal{X} \\ \mathcal{Y} \end{pmatrix} = \begin{bmatrix} A & B \\ C & D \end{bmatrix} \times \begin{pmatrix} x_{\rm corr} - x_\circ \\ y_{\rm corr} - y_\circ \end{pmatrix} + \begin{pmatrix} \mathcal{X}_\circ \\ \mathcal{Y}_\circ \end{pmatrix} \tag{1}$$

where A, B, C, D are the coefficients from the linear transformation that are used to calculate the average rotation angle (θ), the average scale of the transformation (s), and two skew terms (ζ_1, ζ_2), by the following relations:

$$\begin{aligned} \tan(\theta) &= (B-C)/(A+D) \\ s &= \sqrt{AD-BC} \\ \zeta_1 &= (A-D)/2s \\ \zeta_2 &= (B+C)/2s \end{aligned} \tag{2}$$

For each star present in both the master catalog and an individual distortion-corrected frame we have two pairs of coordinates $[(x_{\rm corr}, y_{\rm corr})\ ;\ (\mathcal{X}, \mathcal{Y})]$. For an observation with N stars found in the image and in the master catalog, the list $[(x_{\rm corr}, y_{\rm corr})\ ;\ (\mathcal{X}, \mathcal{Y})]_{i=1,\ldots,N}$ can be used to solve for the parameters in the linear transformation $[A, B, C, D, \mathcal{X}_\circ, \mathcal{Y}_\circ]$ using a linear least-squares fit (see Equation 2 in Anderson (2007)).

According to van der Marel *et al.* (2007), the skew terms ζ_1 and ζ_2 do not separate two effects: neither the difference in scale nor the non-perpendicularity between axes. These effects are due to the fact that the skew in one frame can manifest itself as either ζ_1 or ζ_2 or both, depending on the rotation angle θ between the frames. Thus, we adopt the quantities u and v defined as:

$$\begin{bmatrix} A & B \\ C & D \end{bmatrix} = s \times \begin{bmatrix} \cos\theta & \sin\theta \\ -\sin\theta & \cos\theta \end{bmatrix} \times \begin{bmatrix} 1+v & u \\ u & 1-v \end{bmatrix} \tag{3}$$

i.e., (provided that $u, v \ll 1$) the original matrix of coefficients can be expressed as the product of a pure rotation matrix and a pure skew matrix. Inverting the matrix, these new quantities u and v can be written as functions of the derived parameters A, B, C, and D with:

$$\begin{aligned} u &= \zeta_1 \sin\theta + \zeta_2 \cos\theta \\ v &= \zeta_1 \cos\theta - \zeta_2 \sin\theta \end{aligned} \tag{4}$$

These quantities better disentangle the two effects of difference in scale ($v \neq 0$), and departure from orthogonality ($u \neq 0$) between the two axes. In other words, how much a square is transformed into a rectangle ($v \neq 0$), or into a rhombus ($u \neq 0$) or into a combination of both resulting in a parallelogram ($u \neq 0$ and $v \neq 0$).

The skew terms u and v were parametrized as linear variations with time by Anderson (2007) using the quantities α and β which relate to u and v with the following relationships:

$$\begin{aligned} \alpha &= 2048 \times u \\ \beta &= 2048 \times v \end{aligned} \tag{5}$$

3. Observations

The main calibration field for our study is located about 6.7 arcmin West of the center of globular cluster 47 Tucanae. This calibration field has been observed multiple times through many ACS/WFC filters for both calibration and science purposes. Using the Mikulski Archive for Space Telescopes (MAST), we downloaded the entire database of 47 Tucanae ACS/WFC F606W observations with exposure times longer than 200 seconds. In Table 1 we list each HST Program ID for these images, together with their exposure times and the range of dates of the observations. In summary, we used 272 images.

The automated calibration pipeline `CALACS` (version 8.0.6, 18 Jul 2012) takes care of the basic data reduction (bias, dark, flat–field corrections). We downloaded the flat–fielded images (`_FLT` files), as well as the charge-transfer efficiency (CTE) corrected images (`_FLC` files). The `_FLC` files are data products generated using the pixel–based CTE correction algorithm (PixelCTE v3.2; Anderson & Bedin (2010)).

Program ID	Exposure Time (seconds)	Date Range
9018	690 720 765 765 1200	April–May 2002
9433	10×340	January–February 2003
9648	$15 \times 400 + 4 \times 1100$	January–August 2003
9656	200 240 360 420 450	November 2002 – August 2003
10043	24×400	February–September 2004
10368	24×400	March–August 2005
10569	4×340	October 2005
10730	3×340	March 2006
10737	10×339	November 2005 – August 2006
10771	12×339	November 2005
11397	14×339	July 2009
11677	$117 \times \sim 1400$	January–October 2010
11880	5×400	September 2009
11887	2×339	March–August 2010
12385	6×400	November 2010
12389	3×339	November 2010 – July 2011
12730	6×400	November 2011
12734	3×339	December 2011– July 2012

Table 1: *F606W observations used in this study.*

4. Method

4.1 Photometry and Accurate Source Positions

Positions and fluxes of point sources were accurately measured with the FORTRAN software img2xym_WFC.09x10 in the library of codes by J. Anderson. This code includes the best available geometric distortion solution and is documented and described in detail in Anderson & King (2006).

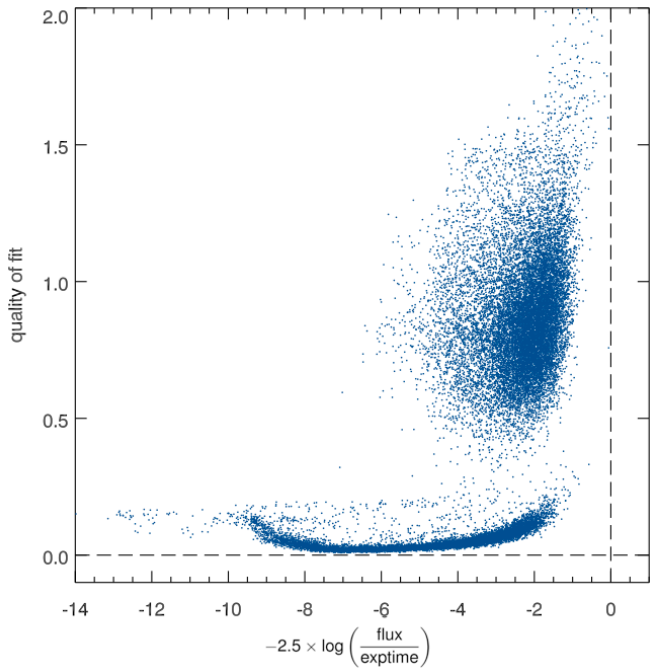

Figure 1: *Typical photometry plot showing the quality of the PSF fit as a function of instrumental magnitude. The real sources are the ones with lower value of* qfit. *In the text we describe how spurious detections were discarded.*

PSF-fitting photometry was performed on all _FLT and _FLC images listed in Table 1 using library PSFs described in Anderson & King (2006). For each image, this task produces an _xym file containing: each source position in the image frame (x,y), its instrumental magnitude, and a quality of fit value (qfit).

The fluxes are corrected for pixel area and converted into instrumental magnitudes ($-2.5\log$(flux)) where the flux is given in units of electrons.

Figure 1 shows the quality of fit (qfit) as a function of instrumental magnitude of all the sources found in image j9irw4azq with exposure time of 339 seconds. Note the presence of false detections such as cosmic rays and hot pixels with qfit$> 0.2-0.3$.

We performed our analysis in both _FLT and _FLC images because of the known effect that imperfect charge transfer in CCDs has upon centroid shifts; see for example Kozhurina-Platais *et al.* (2007).

4.2 Solving for Linear Terms

The next step is to cross-identify the stars in each exposure's _xym file with the stars in the master catalog with coordinates $(\mathcal{X},\mathcal{Y})$. To do this, we used a pattern-matching algorithm that matches pairs of coordinates in two lists based on triangles that can be formed from groups of three points in each list.

The (x,y) coordinates from each observation are corrected for geometric distortion using the special solution for filter F606W yielding the new coordinates $(x_{\rm corr}, y_{\rm corr})$ which are then matched to the already corrected master catalog coordinates $(\mathcal{X},\mathcal{Y})$. The distortion solution used for this has no time dependency in its skew terms.

This process provides a first approximation linear transformation that includes all the matched stars, including false detections matched with real reference frame stars. The left panel in Figure 2 shows an example residual plot for image `j9irw4azq_flt`.

Two groups of stars are clearly seen in this plot. The group in the center contains stars that are members of 47 Tucanae. The off-centered group corresponds to Small Magellanic Cloud (SMC) stars. This separation is caused by the observed proper motion of the 47 Tucanae globular cluster relative to that of the SMC. This effect is also described in Kozhurina-Platais *et al.* (2009). In order to have a clean sample of stars for our study, we only selected sources that are from 47 Tucanae and that had position residuals less than 0.07 WFC pixel ($\sim$ 3.5 mas) in radius. Those objects are shown in red. Their corresponding photometry is presented in the right panel in Figure 2. This procedure allows us to reject false detections like cosmic rays and hot pixels, as well as non-members of the cluster. The final star selection is thus very clean and reliable.

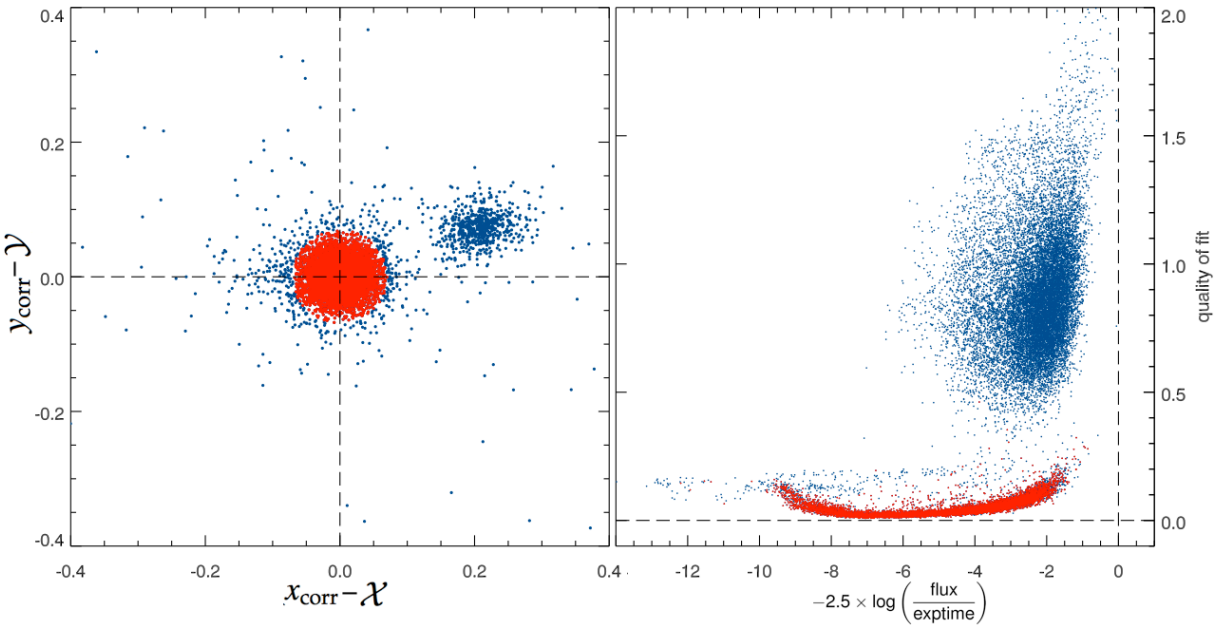

Figure 2: [Left] *Plot showing position residuals measured using image* `j9irw4azq_flt` *and the reference catalog. The stars used for the final least–square fitting are those shown in red. The units are* ACS/WFC *pixels.* [Right] *Same as Figure 1, with the same color coding as in the left panel.*

We refined our solutions for the parameters A,B,C, and D by running the least square fit a second time on `_FLT` and `_FLC` images using only the selected stars within a radius of 0.07 WFC pixels. With these parameters we were able to compute the values of the skew terms defined in Equation 4.

5. Analysis and Results

Using the estimated parameters A, B, C, and D we calculated the skew terms (u and v) according to Equation 4. Figure 3 shows the skew terms as a function of time. Their radian values have been scaled by 2048 to convert into WFC pixels at the extreme edge of the detector. The values shown were derived from the _FLT images; very similar results were derived from the _FLC images. The dark-blue points represent pre-SM4 observations and the light-blue points represent post-SM4 images. This applies to all Figures in this ISR.

Both sets of points show a linear trend with time. This is a known result that was already found by Anderson (2007) and van der Marel *et al.* (2007) for the pre-SM4 data. We fit a simple linear function to the data and found the solution given in Equation 6:

$$\texttt{FLT images} \quad \left| \begin{array}{rl} 2048 \cdot u(\texttt{time}) = & 0.095 + 0.088 \times (\texttt{time} - 2004.5)/2.5 \\ 2048 \cdot v(\texttt{time}) = & -0.028 - 0.034 \times (\texttt{time} - 2004.5)/2.5 \end{array} \right. \tag{6}$$

where time is expressed in units of years.

This fit represents the pre-SM4 trend very well and is in agreement with the previous work by Anderson (2007). We fit a similar function to the u and v pre-SM4 values obtained using _FLC images, and the new simple corrections are given in Equation 7.

$$\texttt{FLC images} \quad \left| \begin{array}{rl} 2048 \cdot u(\texttt{time}) = & 0.092 + 0.088 \times (\texttt{time} - 2004.5)/2.5 \\ 2048 \cdot v(\texttt{time}) = & -0.024 - 0.030 \times (\texttt{time} - 2004.5)/2.5 \end{array} \right. \tag{7}$$

Post-SM4 data show a similar trend but are clearly displaced by the time that the ACS was out of service since January 2007 (camera failure) through May 2009 (Servicing Mission 4).

We fit the post-SM4 data obtained with both the _FLT and _FLC images and the new solutions for u and v as a function of time are given by Equations 8 and 9.

$$\texttt{FLT images} \quad \left| \begin{array}{rl} 2048 \cdot u(\texttt{time}) = & 0.229 + 0.070 \times (\texttt{time} - 2011.0)/2.0 \\ 2048 \cdot v(\texttt{time}) = & -0.088 - 0.044 \times (\texttt{time} - 2011.0)/2.0 \end{array} \right. \tag{8}$$

$$\texttt{FLC images} \quad \left| \begin{array}{rl} 2048 \cdot u(\texttt{time}) = & 0.230 + 0.070 \times (\texttt{time} - 2011.0)/2.0 \\ 2048 \cdot v(\texttt{time}) = & -0.074 - 0.037 \times (\texttt{time} - 2011.0)/2.0 \end{array} \right. \tag{9}$$

In order to verify our method and the new post-SM4 set of corrections, we solve the linear system in Equation 1 on the _FLT images again, but this time we turn on the skew time-dependency

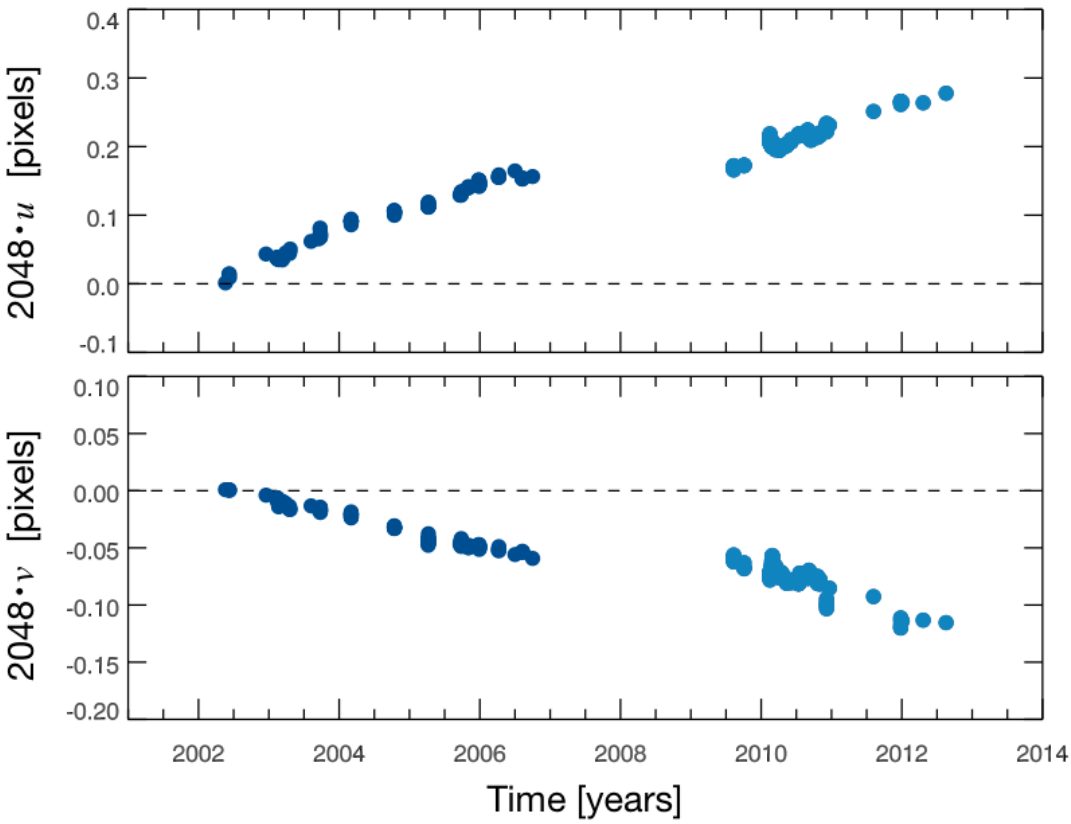

Figure 3: *The trends in the two skew terms against time. No time-dependent correction applied. The dark-blue points represent pre-SM4 observations and the light-blue points represent post-SM4 images. The scaling by 2048 provides the size of the effect in pixels at the edge of the detector.*

correction as shown in Equations 6 and 8. The corrected u and v values are presented in Figure 4. For comparison, we over plotted the un-corrected observations using gray points. The time-dependent skew corrections flatten the distributions. Both post-SM4 and pre-SM4 time-corrected data show no trend whatsoever. The skew terms u and v calculated for images observed in 2012 show similar values as those estimated for images observed close to the ACS installation in 2002.

In Figure 5 we present the skew terms ζ_1 and ζ_2 (in units of WFC pixels) as a function of time. The left panels show the results obtained for the `_FLT` images with no time-dependent correction. The plots on the right side show ζ_1 and ζ_2 after the linear correction was applied. These residual terms show some variations with time, but the amplitude of this variation is very small (less than 0.02 WFC pixel) compared to what was seen before the correction (0.3 pixel).

We also analyzed possible variations of the skew terms as a function of the telescope roll-angle, as specified by the image header keyword `PA_V3`. In this analysis we have adopted the definition for the skew term given by Kozhurina-Platais & Petro (2012) as in Equation 10

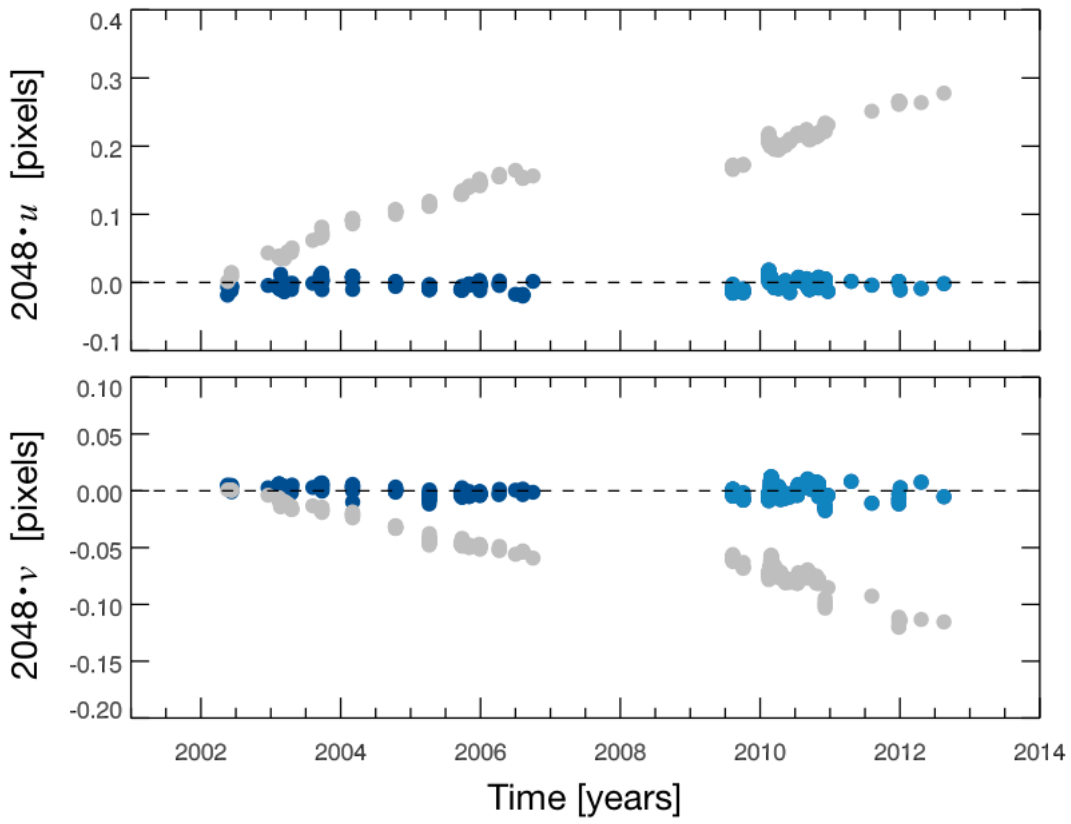

Figure 4: *The trends in the two skew terms against time for* `_FLT` *images. The new time-dependent corrections were applied. The dark-blue points represent pre-SM4 observations and the light-blue points represent post-SM4 images. Gray points represent the original un-corrected data. It is shown to aid the eye in the comparison. The scaling by 2048 provides the size of the effect in pixels at the edge of the detector.*

$$\tan(\gamma) = -\frac{AB+CD}{AD-CB} \tag{10}$$

When no correction is applied, the left panel in Figure 6 shows a clear sinusoidal trend with large amplitude of γ, up to as much as 60". However, if the skew time-dependent correction is applied, then the skew shows no trends and varies by at most 5".

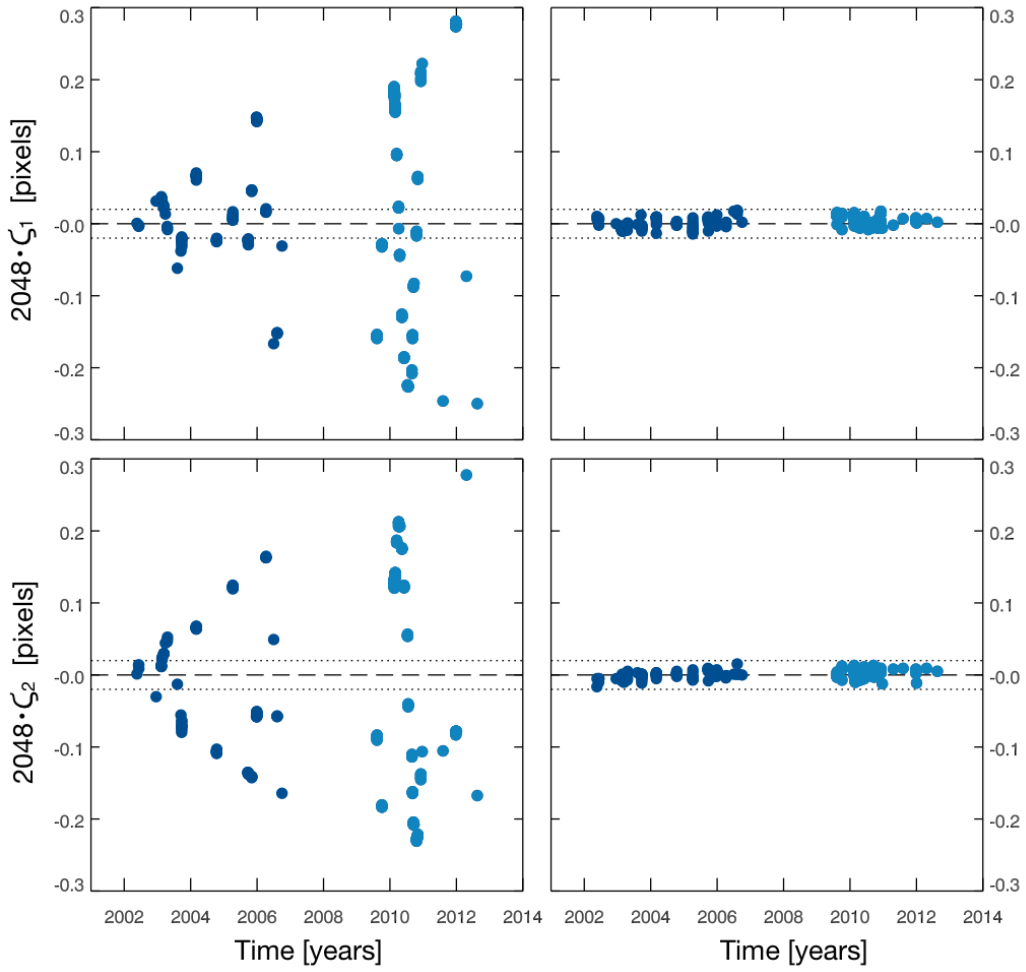

Figure 5: *The trends in the two skew terms:* ζ_1 [Above] *and* ζ_2 [Below] *against time for* _FLT *images.* [Left] *No time-dependent correction applied.* [Right] *Data has been corrected with the new linear corrections. The amplitude of the remaining variation is smaller than 0.02* WFC *pixels (shown as a dotted line in both figures). The scaling by 2048 provides the size of the effect in pixels at the edge of the detector.*

6. Conclusions

We re-visit the problem of the time dependency of the linear terms in the ACS/WFC geometric distortion. The first solution to this problem was provided by Anderson (2007) and it only applied to pre-SM4 _FLT images.

We performed a study of the variability of the linear terms of the distortion of the ACS/WFC CCDs using the calibration field close to the center of globular cluster 47 Tucanae. We extended the study to post-SM4 observations and we analyzed both _FLT and _FLC F606W images. We provide new and simple corrections that will allow observers to perform global astrometric studies with 0.02 WFC pixel precision.

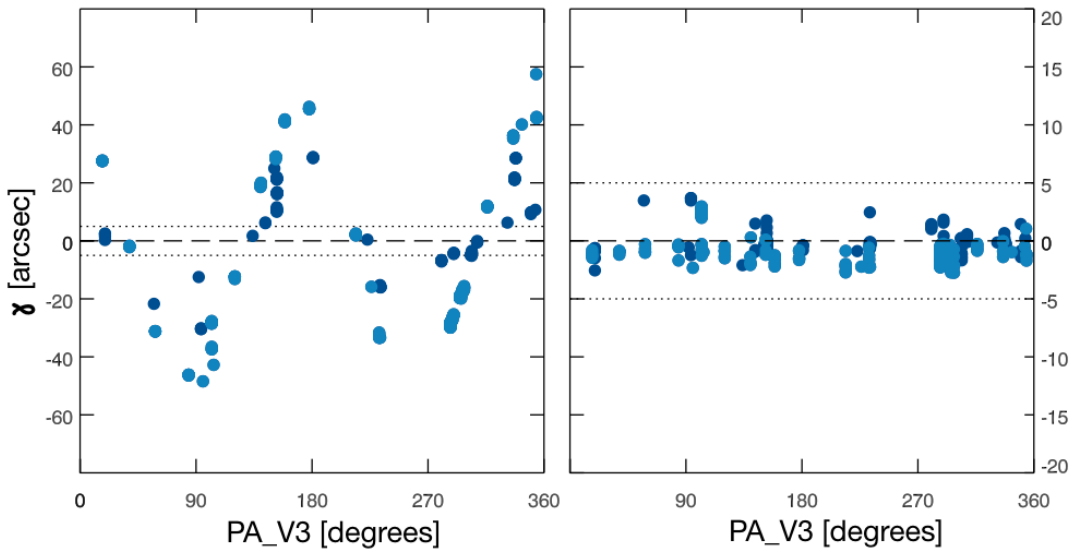

Figure 6: *Skew (γ) in arcsec as a function of the parameter* `PA_V3` *which is recorded as a science header keyword.* [Left] *No time-dependent correction applied.* [Right] *Data has been corrected with the new linear corrections. The amplitude of the remaining variation is smaller than 5 arcsec (shown as a dotted line in both figures).*

The corrections are presented as linear functions of the form:

$$\begin{aligned} 2048 \cdot u(\texttt{time}) &= u_1 + u_2 \times (\texttt{time} - t_0)/u_3 \\ 2048 \cdot v(\texttt{time}) &= v_1 + v_2 \times (\texttt{time} - t_0)/v_3 \end{aligned} \tag{11}$$

where `time` is the date of the observation expressed in years, t_0 is an arbitrary parameter equal to 2004.5 for pre-SM4 data and 2011.0 for post-SM4 data. The coefficients u_1, u_2, v_1, v_2 and their errors are listed in Table 2. The coefficients u_3 and v_3 are also fixed and equal to 2.5 and 2.0 for pre-and post-SM4 data respectively. The scaling by 2048 provides the size of the effect in units of WFC pixels at the edge of the detector.

We also studied possible variations of the skew as a function of the telescope roll-angle and found that the new corrections completely erase a sinusoidal trend found when no time-correction is applied.

	u_1	u_2	v_1	v_2
		Pre-SM4 observations		
FLT	0.095 ± 0.004	0.088 ± 0.002	-0.028 ± 0.001	-0.034 ± 0.002
FLC	0.092 ± 0.001	0.088 ± 0.001	-0.024 ± 0.001	-0.030 ± 0.001
		Post-SM4 observations		
FLT	0.229 ± 0.001	0.070 ± 0.002	-0.088 ± 0.001	-0.044 ± 0.002
FLC	0.230 ± 0.001	0.070 ± 0.002	-0.074 ± 0.001	-0.037 ± 0.002

Table 2: *Values of the coefficients in the linear functions in Equation 11.*

Acknowledgments

The authors would like to thank N. Grogin and J. Anderson for their comments and revision suggestions that resulted in an improvement of this work. The authors acknowledge very helpful conversations with N. Dencheva and W. Hack. Finally, we are grateful to J. Anderson for providing access to his suite of FORTRAN algorithms.

References

Anderson, J. 2002, *HST Calibration Workshop: Hubble after the Installation of the ACS and the NICMOS Cooling System*, 13

Anderson, J., & King, I. R. 2006, *Instrument Science Report* ACS 2006–01

Anderson, J. 2007, *Instrument Science Report* ACS 2007–08

Anderson, J., & Bedin, L. R. 2010, PASP , **122**, 1035

Kozhurina-Platais, V., Goudfrooij, P. & Puzia, T. H. 2007, *Instrument Science Report* ACS 2007–04

Kozhurina-Platais, V., Cox, C., McLean, B., *et al.* 2009, *Instrument Science Report* WFC3 2009–33

Kozhurina-Platais, V., & Petro, L. 2012, *Instrument Science Report* WFC3 2012–03

Meurer, G. R., Lindler, D., Blakeslee, J. P., *et al.* 2002, *HST Calibration Workshop: Hubble after the Installation of the ACS and the NICMOS Cooling System*, 65

van der Marel, R. P., Anderson, J., Cox, C., *et al.* 2007, *Instrument Science Report* ACS 2007–07